JOURNAL OF GEOPHYSICAL RESEARCH, VOL. 115, D13101, doi:10.1029/2009JD013114, 2010

A discussion of the links between solar variability and high-storm-surge events in Venice

David Barriopedro,[1] Ricardo García-Herrera,[2] Piero Lionello,[3] and Cosimo Pino[3]

Received 31 August 2009; revised 8 January 2010; accepted 16 February 2010; published 1 July 2010.

[1] This study explores the long-term frequency variability of high-surge events (HSEs) in the North Adriatic, the so-called *acqua alta*, which, particularly during autumn, cause flooding of the historical city center of Venice. The period 1948–2008, when hourly observations of sea level are available, is considered. The frequency of HSEs is correlated with the 11 year solar cycle, solar maxima being associated with a significant increase in the October-November-December HSE frequency. The seasonal geopotential height pattern at 1000 hPa (storm surge pattern; SSP) associated with the increased frequency of HSEs is identified for the whole time period and found to be similar to the positive phase of the main variability mode of the regional atmospheric circulation (empirical orthogonal function 1; EOF1). However, further analysis indicates that solar activity modulates the spatial patterns of the atmospheric circulation (EOF) and the favorable conditions for HSE occurrence (SSP). Under solar maxima, the occurrence of HSEs is enhanced by the main mode of regional atmospheric variability, namely, a large-scale wave train pattern that is symptomatic of storm track paths over northern Europe. Solar minima reveal a substantially different and less robust SSP, consisting of a meridionally oriented dipole with a preferred southward path of storm track activity, which is not associated with any dominant mode of atmospheric variability during low-solar periods. It is concluded that solar activity plays an indirect role in the frequency of HSEs by modulating the spatial patterns of the main modes of atmospheric regional variability, the favorable patterns for HSE occurrence, and their mutual relationships, so that constructive interaction between them is enhanced during solar maxima and inhibited in solar minima.

Citation: Barriopedro, D., R. García-Herrera, P. Lionello, and C. Pino (2010), A discussion of the links between solar variability and high-storm-surge events in Venice, *J. Geophys. Res.*, *115*, D13101, doi:10.1029/2009JD013114.

1. Introduction

[2] In recent years the Venice lagoon has received much attention as a case of coastal vulnerability, mainly because of relative sea level rise and increased frequency of flooding. Instrumental records of local tide gauges provide a mean relative sea level rise of 2.4 mm year^{-1} for the period 1872–2005 [*APAT*, 2006]. This increase is higher than that estimated from archeological evidence for 200–1400 AD [1.3 mm yr^{-1}; *Ammerman and McClennen*, 2000] and from proxy-based reconstructions over the last three centuries [1.9 mm yr^{-1}; *Camuffo and Sturaro*, 2003]. Several factors contribute to such an increase: (1) mean sea level rise caused by global warming (thermal expansion of oceans and increased melting of glaciers and ice caps), (2) regional changes in water temperature and salinity caused by modifications of air-sea fluxes and precipitation patterns, and (3) local land subsidence due to geological processes and anthropogenic activities, the most important one being the pumping of coastal groundwater, which caused subsidence rates of ~2.5 mm yr^{-1} between 1930 and 1970 [e.g., *Camuffo*, 1993; *Pirazzoli and Tomasin*, 2002; *Zanchettin et al.*, 2007].

[3] Within this context of mean sea level rise, the city of Venice has experienced an increasing frequency of storm surges during the second half of the 20th century [*Pirazzoli*, 1991; *Camuffo*, 1993]. The astronomical tide alone (between 25 and 80 cm) is unable to flood the city; rather, flooding events in Venice are the result of severe meteorological conditions, sometimes amplified by a high astronomical tide level or free oscillations of the Adriatic Sea. The triggering factor is the passage of deep low-pressure systems that cause sea level pressure (SLP) gradients and strong Sirocco (southeasterly) winds along the Adriatic Sea, which determine the piling-up of water at the northern end of the basin [*Pirazzoli and Tomasin*, 1999; *Trigo and Davies*, 2002; *Lionello*, 2005]. Because Sirocco winds, together with Bora (northeasterly) winds, characterize the climatological regional background from October to January, sea surges in the Venice lagoon are typical during this time of the year.

[1]CGUL-IDL, Faculdade de Ciências, Universidade de Lisboa, Lisbon, Portugal.
[2]Departamento Física de la Tierra II, Facultad de Ciencias Físicas, Universidad Complutense de Madrid, Madrid, Spain.
[3]Department of Material Science, University of Salento, Lecce, Italy.

0148-0227/10/2009JD013114

[4] Reconstructions back to the eighth century [*Camuffo*, 1993] indicate the existence of anomalous periods in the frequency of sea surges (particularly recurrent in the first halves of the 16th and 18th centuries) and a continuous positive trend during the second half of the 20th century, which has been an unprecedented period of frequent and intense floods. Long-term variability in the frequency of floods has been attributed partially to interannual fluctuations of some large-scale climate patterns, which favor the occurrence of the meteorological conditions determining the storm surge in the North Adriatic. In particular, the North Atlantic Oscillation (NAO) has been reported to exert an influence on the Adriatic Sea level through modulation of (1) atmospheric pressure anomalies that induce the hydrostatic barometric response of water masses and (2) hydrological budgets in the Adriatic Sea and in bordering areas, mainly freshwater river input from the Po River runoff [e.g., *Tsimplis and Josey*, 2001; *Zanchettin et al.*, 2006]. However, whereas the NAO index is negatively correlated with the frequency and magnitude of winter sea surges, its influence during autumn, when most of the city floods occur, is limited [*Fagherazzi et al.*, 2005]. Thus, further analyses of the long-term variability of sea surges and the relationship to climate variability are required to understand changes in the frequency of surge events.

[5] Solar activity, typically measured by the number of sunspots, has also been proposed as a feasible candidate for affecting flooding variability. *Camuffo et al.* [2000] and *Camuffo and Sturaro* [2004] tested this linkage at centennial time scales by analyzing a millennial reconstruction of floods in Venice. They found a peak in flooding frequency during the Spörer Minimum (1416–1534) of solar activity; in contrast, other periods of anomalous low solar activity, such as the Oort Minimum (1010–1090), the Wolf Minimum (1282–1342), and the Maunder Minimum (1645–1715), revealed no similar increase. They concluded that a link between flooding and sunspots was improbable or was masked by other factors in this region.

[6] Variations in solar radiation, however, have a wide range of temporal scales, the most important at interannual-interdecadal time scales being the 11 year solar cycle. Several studies have noticed the similarity between the 11 year solar cycle and flood surge activity in Venice [*Smith*, 1986; *Tomasin*, 2002; *Lionello*, 2005], but have not addressed this question in detail. Such a linkage is not totally surprising, given that the 11 year solar cycle has significant effects on several variables in the troposphere, including surface temperatures, geopotential height, position of low-pressure-system centers [*Christoforou and Hameed*, 1997; *van Loon and Shea*, 1999; *Gleisner and Thejll*, 2003; *Balling and Roy*, 2005; *Gleisner et al.*, 2005], and the spatial patterns of tropospheric circulation variability [*Kodera*, 2002; *Huth et al.*, 2006]. The increasing evidence of solar effects in the troposphere suggests the existence of a physical mechanism capable of amplifying the small changes in input energy caused by the 11 year solar cycle. Recent investigations have reported a detectable atmospheric response to the 11 year solar cycle via radiative-photochemical (UV-ozone) processes that induce temperature and zonal wind anomalies in the tropical upper stratosphere [e.g., *Shindell et al.*, 1999; *Lean and Rind*, 2001]. While the existence of a solar signal in the tropical stratosphere is well established, the understanding of solar effects in the extratropical troposphere remains controversial. Some authors have provided dynamical arguments in terms of a poleward propagation of the tropical stratospheric zonal wind anomalies and a subsequent downward propagation in extratropics [*Kodera and Kuroda*, 2002; *Baldwin and Dunkerton*, 2005; *Matthes et al.*, 2006], although there is no satisfactory theory explaining these events yet. This mechanism is also known to communicate the quasi-biennial oscillation to the high-latitude stratosphere [e.g., *Labitzke*, 2005].

[7] Here the long-term variability of high-surge events (HSEs) is analyzed, aiming at the identification of its modulation by the 11 year solar cycle. More specifically, the objectives of this study are (1) to explore the interannual-interdecadal variability of HSEs; (2) to identify the atmospheric general circulation pattern responsible for the occurrence of HSE at these time scales; and (3) to assess their linkage with the 11 year solar cycle. The paper is organized as follows: section 2 describes data sources and the definition of HSEs. Section 3 explores the variability of HSEs and the relationship to solar activity, focusing on the solar modulation of atmospheric variability and the favorable conditions for HSE occurrence. Results are discussed in section 4. Finally, the last section summarizes the main conclusions.

2. Data

[8] The analysis carried out in this study uses hourly sea level values, geopotential height fields, and estimates of solar irradiance. Hourly values of sea level (cm) for the 1948–2008 period were provided by the Ufficio Idrografico (Hydrographic Office) of Venice for the tide gauge of Punta della Salute in Venice. This data set is used to identify single independent storm surge events. The first step consists of removing the astronomical tide effect and the mean sea level to obtain a time series that includes only the effect of surges and seiches. These are the normal modes of oscillation of the basin, with periods of about 22 and 11 h that typically disappear 3–4 days after the passage of a storm. To include in the statistics only independent events, a minimum 72 h separation is required among peak sea level values, since floods can also be caused by seiches triggered by a previous surge [*Robinson et al.*, 1973]. Thus, in the hourly time series, isolated peaks and the successive seiches are attributed to a single storm surge event. The strength and time of occurrence of each event are given by the magnitude and time of maximum sea level, respectively. This work considers only HSE, defined as those events in which maximum sea level exceeds the 95th percentile (69 cm) of the total distribution.

[9] Daily and monthly fields of geopotential height at 1000 hPa (Z1000) and 2.5° × 2.5° grid resolution were extracted from the National Centers for Environmental Prediction (NCEP)/ National Center for Atmospheric Research reanalysis [*Kalnay et al.*, 1996] for the period 1948–2008 and the region (20, 85)°N and −60°W, 60°E.

[10] Annual data on the full solar disc 10.7 cm radio flux (in solar flux units; 1 sfu = 10^{-22} W m^{-2} Hz^{-1}) were obtained from the National Geophysical Data Center of the National Oceanic and Atmospheric Administration (NOAA). Solar radio flux emissions at 2800 MHz frequency (or 10.7 cm wavelength) integrated for the solar disc are usually employed

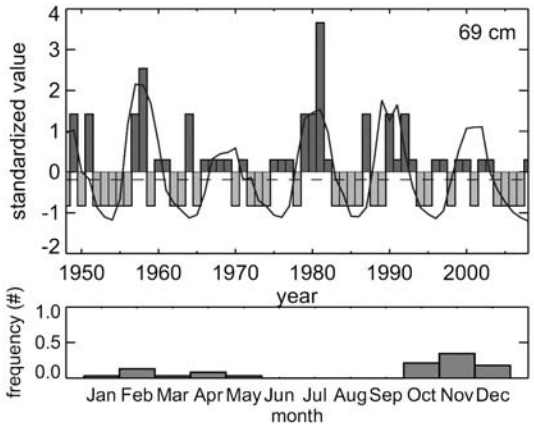

Figure 1. Long-term time series and mean annual cycle of high-surge events (HSEs) in Venice. (top) Standardized time series of annual 10.7 cm radio flux (solid line) and October-November-December (OND) HSEs in Venice (bars) defined as surge events above 69 cm (95th percentile) separated by at least 72 h. The dashed line indicates the median of the annual solar series separating high solar (HS) and low solar (LS) years. (bottom) The 1948–2008 climatological annual cycle of the frequency of HSEs.

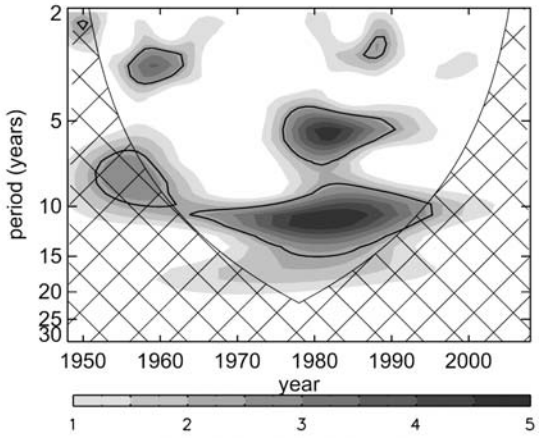

Figure 2. Dominant periodicities in the seasonal time series of HSEs. Wavelet spectrum of the Morlet type for the frequency series of OND HSEs. Shaded areas indicate the power/variance ratio. Cross-hatched areas denote the cone of influence. Solid lines reflect significant oscillation bands at the $p < 0.1$ level.

to monitor solar radiant energy, as they belong to the spectral range that correlates better with the total solar irradiance and with the sunspot number [e.g., *Tapping and Charrois*, 1994].

[11] Since the period of study includes 61 years, this means almost six and a half solar cycles, with six periods of high and six periods of low solar activity, respectively. The two groups of years above and below the median of solar activity contain a set of 30 years each, designated high solar (HS) and low solar (LS), respectively. As this stratification does not allow for neutral years, HS (LS) years are also referred to as solar maxima (minima).

[12] The methodological approach is based on principal component analysis (PCA) and associated empirical orthogonal functions (EOFs). Spearman's rank correlations, denoted r (p is the significance level), and composite differences have also been employed, the statistical significance being tested with a Spearman's rho correlation test and a two-tailed t-test, respectively.

3. Results

3.1. Long-Term Variability of High-Surge Event (HSE) Frequency

[13] The monthly mean frequency of HSE for the 1948–2008 period is shown in the lower plot in Figure 1. The climatological maximum occurs between October and December (~75% of all cases). The annual time series with the total frequency of HSEs during October-November-December (OND) (bars in the upper plot in Figure 1) does not show a significant trend, since the effect of sea level rise and ground subsidence has been removed by subtracting the mean sea level. However, there is large interdecadal variability in the occurrence of HSEs, which seems to be in good correspondence with the 11 year solar cycle (solid line; Figure 1). In fact, the time series of solar activity and OND HSEs show significant correlations ($r = 0.30$, $p < 0.05$) for the 1948–2008 period. A wavelet analysis applied to the OND HSE series (Figure 2) reveals that the variability of surge event activity is mainly dominated by significant periodicities near the 11 year bands, which reach statistical significance for the period between the 1960s and 1990s, but it is associated with an enhancement of power spectrum variance throughout most of the record. These results are suggestive of an 11 year solar signal.

[14] The possible influence of solar activity is further explored in Figure 3, which shows the annual cycle of HSE frequency for HS and LS years and for the whole time

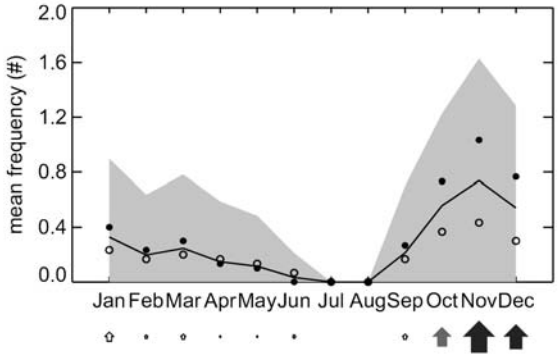

Figure 3. Solar signal in the annual cycle of HSE occurrence. Shaded contours indicate the 0.5σ level of the monthly mean (solid line). Filled and open circles represent the composite for HS and LS years, respectively. The size of the arrows is proportional to the difference between HS and LS frequency in HSEs. Light arrow and dark-shaded arrows indicate significant differences at the $p < 0.1$ and $p < 0.01$ level, respectively. White arrows represent no significant differences.

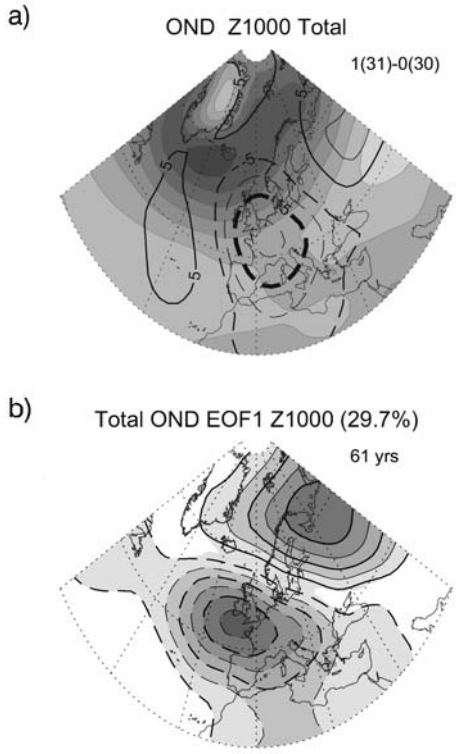

Figure 4. Seasonal patterns associated with HSEs and the dominant mode of atmospheric circulation. (a) Three-month averaged OND Z1000 pattern associated with HSEs, in geopotential meters (gpm). Lines indicate the composite difference between years with at least one event and years without any event in OND. Solid (dashed) lines indicate positive (negative) differences. Bold lines denote differences significant at $p < 0.05$. Shaded areas represent the climatological OND Z1000 field with CI 25 gpm starting at 0 gpm (dark). (b) First EOF of the OND Z1000 anomaly time series for 1948–2008. Solid (dashed) lines indicate positive (negative) normalized loadings.

period. To avoid sampling problems, HSE frequencies are computed for each month by using 3 month centered running windows. HS activity is significantly associated with higher frequencies of HSE between October and December. As a consequence, subsequent analyses focus on the frequency of HSEs during the OND season (hereafter, autumn), and hence, from now on the term HSE refers exclusively to the frequency of OND HSEs. It should be stressed here that the link to solar activity is restricted to HSEs, not to all surge events. Further analysis (not shown) has revealed that the signal is still appreciable when HSEs are defined from the 90th percentile rather than the 95th percentile, but it weakens for lower thresholds.

3.2. Seasonal Patterns Associated with HSE Frequency Variability

[15] As explained before, sea surge events in Venice are triggered by the passage of deep cyclones, which are related to the intensity and position of the storm track over western Europe and, hence, to the sea level pressure pattern. Therefore, it could be asked whether autumns with enhanced or reduced HSE activity are associated with specific anomalous circulation patterns. To address this question, the difference between two Z1000 composites, one for years with at least one HSE in the OND period and the other for those years without any HSE, has been computed (Figure 4a). These seasonal composites are representative of active and quiet years, respectively, as far as seasonal HSE activity is concerned. The threshold of one surge event was chosen to provide a balanced sample size between the two composites.

[16] The associated pattern presents a center of action located above western Europe and suggests the penetration of cyclones into the Mediterranean region during periods with frequent HSEs. These results are in agreement with previous studies [*Lionello*, 2005] and with a complementary analysis performed in the 2–6 day band-pass-filtered Z1000 variance (not shown), which reveals an enhancement of storm track activity over that region. From now on the pattern in Figure 4a is referred to as the storm surge event pattern (SSP), bearing in mind that it is associated with a seasonal mean configuration that enhances the occurrence of HSE in Venice. The time series of the score obtained by projecting OND Z1000 anomalies (computed relative to the mean field of the 1948–2008 period) onto the normalized SSP in Figure 4a shows a significant correlation ($r = 0.35$, $p < 0.01$) with the time series of OND HSEs.

[17] Note that SSP does not resemble the traditional meridional NAO dipole but, rather, a wave train pattern. These results are in agreement with *Fagherazzi et al.* [2005] and *Lionello* [2005], who found no important link between the classical NAO and HSEs in Venice during autumn. The immediate question that follows is whether SSP has a correspondence with any other mode of atmospheric variability. To address this question, an EOF analysis has been applied to the covariance matrix of the seasonal OND anomalies weighted by the square of the cosine of latitude. A measure of the similarity between spatial patterns is given by the normalized projection index (PI) of the EOF pattern onto the SSP:

$$\mathrm{PI} = \frac{\langle Z_{\mathrm{EOF}}, Z_{\mathrm{SSP}} \rangle}{\langle Z_{\mathrm{SSP}}, Z_{\mathrm{SSP}} \rangle}, \tag{1}$$

where the angle brackets indicate the normalized projection, and Z represents the Z1000 loading matrix for either the EOF pattern or the SSP.

[18] Among the first five EOFs (>85% of the total variance), only the first one (Figure 4b; 29.7% of the explained variance) projects remarkably onto the SSP (PI = 0.67). The correlation coefficient between the principal component (PC) of the first EOF (PC1) and the time series of SPP is 0.86 ($p < 0.01$), suggesting that they reflect similar regional patterns. Note that the first EOF does not correspond to the classical NAO pattern either, but it shares more common features with the Scandinavian pattern or the Eurasia-1 pattern, as defined by *Barnston and Livezey* [1987].

[19] To maximize the sample size of HSE and, hence, the robustness of the composite analysis, seasonal patterns are employed herein, with the awareness of filtering out specific monthly features. The main results of this study, however, do not depend crucially on this choice (see section 4).

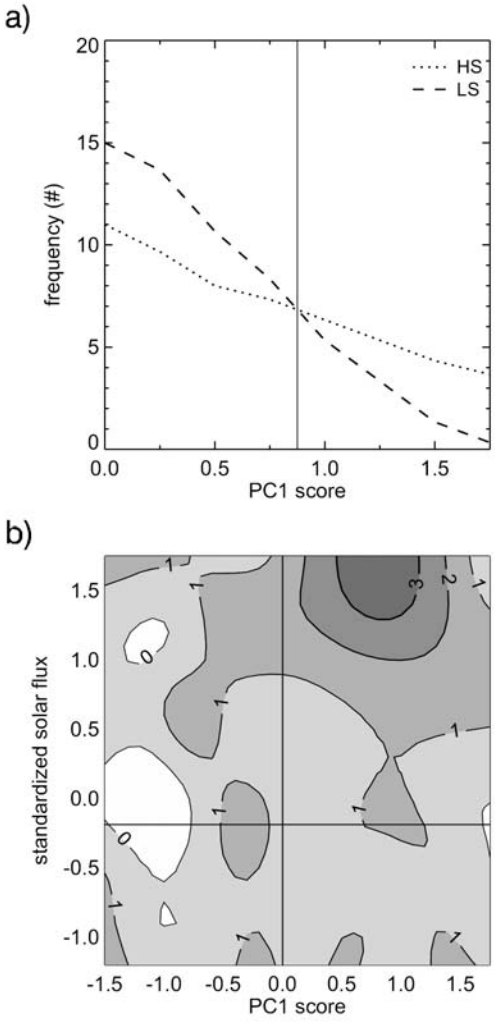

Figure 5. Solar modulation of the linkage between the dominant mode of atmospheric circulation and the frequency of HSEs. (a) Cumulative histogram (i.e., number of years equal to or greater than a given bin) for the positive phases of EOF1 (see Figure 4b) during HS (dotted line) and LS (dashed line) years. (b) Contour plot of the frequency OND HSE versus OND PC1 and annual solar flux. The solar radio flux is standardized. A distance-weighted minimum-curvature spline surface is fitted to the data points. Only PC1 scores with at least one HSE for both HS and LS phases are shown.

3.3. Solar Modulation of the Seasonal Modes of Atmospheric Circulation

[20] Recent investigations have reported detectable solar effects in the spatial patterns of specific weather regimes [e.g., *Barriopedro et al.*, 2008] and of some modes of tropospheric variability [e.g., *Kodera*, 2002; *Huth et al.*, 2006]. Therefore, a possible explanation for the observed solar signal in the frequency of HSEs could be provided in terms of a solar modulation of the dominant mode of atmospheric variability. Such an influence may occur through (1) the amplitude of the EOF1, so that positive phases of the PC1 would be especially recurrent in HS periods, or (2) the spatial pattern of the EOF1, so that the SSP would not find a favorable mode in solar minima. Note that hypothesis 1 adopts a global EOF1 that is independent of solar activity (i.e., the EOF1 pattern is the same regardless of solar activity). Conversely, hypothesis 2 requires a solar modulation of atmospheric circulation (i.e., the EOF1 changes its spatial pattern under solar activity).

[21] To explore hypothesis 1, a cumulative frequency histogram with the positive phases of the PC1 has been plotted for HS and LS years (Figure 5a). The distribution is asymmetric, low (high) PC1 values being more frequent during LS (HS) years. Since the SSP is rather similar to the positive phase of the EOF1, the favorable conditions for HSE occurrence are expected to be more frequent in HS years. Conversely, the shape of the seasonal PC1 distribution during LS years, in which almost no cases have PC1 above ~1, suggests that seasonal anomalies in LS years do not significantly project onto the EOF1, and hence, this pattern may not represent a recurrent mode of variability in solar minima.

[22] According to hypothesis 1 the higher frequency of HSE in solar maxima is due to a higher frequency of the positive values of PC1, and hence, the statistical linkage between HSE and PC1 would be independent of the solar activity (i.e., positive phases of EOF1 would enhance the occurrence of HSEs equally in both solar phases). Figure 5b shows the simultaneous role of solar activity and PC1 (independent variables) in HSE (dependent variable), in a plot of the frequency of HSEs for each year in the 1948–2008 period against its PC1 score and its level of solar activity. The maximum frequency of HSE occurs under the simultaneous conditions of HS activity and positive phases of the PC1. However, there does not seem to be any dependence between PC1 and HSEs in LS years. In fact, the correlations between them reveal a significant relationship for HS years ($r = 0.34, p < 0.05$) that weakens during LS years ($r = 0.20$; $p < 0.1$, not significant). Thus, the unbalanced frequency of HSEs during opposite solar phases is not due solely to the different recurrence of positive PC1 scores; rather, the HSE-PC1 relationship seems to be a function of the solar activity too. These results suggest a solar modulation beyond the amplitude of EOF1.

[23] To explore hypothesis 2, the PCA has been applied separately to HS and LS years, producing a set of LS-EOFs and HS-EOFs. Note that this solar-stratified analysis allows exploration of changes in the recurrence of the EOFs (via their explained variance) and also changes in the spatial configuration of the EOF patterns related to solar activity. The HS-EOF1 mode (36.1% of explained variance; Figure 6a) resembles the counterpart EOF obtained for all years (Figure 4b) and the SSP. However, the LS-EOF1 (Figure 6b) is not similar to the SSP. Instead, the LS EOF2 (explained variance, 21.6%) pattern best resembles the SSP in solar minima (not shown). These results are in agreement with the lower frequency of SSP-like patterns obtained from the global EOF1 during LS years (Figure 5a).

[24] In addition to the solar unbalance of variances explained by SSP-related EOFs, the PI of the solar-based EOFs onto the SSP reveals values of 0.67 for HS-EOF1 but only 0.47 for LS-EOF2. This is because the characteristic EOF pattern during LS years is shifted to the northeast compared to the SSP, and the negative loading

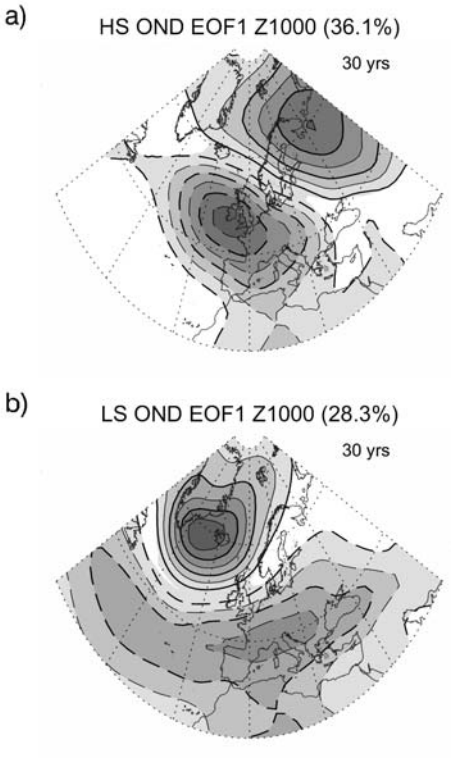

Figure 6. Solar modulation of the dominant pattern of atmospheric circulation. First empirical orthogonal functions (EOF1s) of the OND Z1000 anomaly time series for (a) HS years and (b) LS years. Solid (dashed) lines indicate positive (negative) normalized loadings.

center is located farther north, between the British Islands and the Scandinavian Peninsula (not shown). As a consequence of this weaker SSP-EOF resemblance in solar minima, a larger fraction of SSP variance is explained by HS-PC1 (r^2 = 77.4%) than by LS-PC2 (r^2 = 39.7%). Furthermore, correlations between the PCs of the SSP-related EOFs and the frequency of HSEs are significant during HS activity (r = 0.35, $p < 0.05$), but they vanish in LS years (r = 0.18, p = not significant), for which the likelihood of HSE occurrence is only marginally enhanced, and not tightly tied to any mode. Thus, during LS years the SSP does not find a supporting mode capable of significantly enhancing the occurrence of HSE. These results suggest a solar modulation in the spatial patterns of atmospheric variability, with HS-EOF1 revealing a stronger resemblance to the global SSP and a higher recurrence (or explained variance) than its LS-EOF counterparts.

3.4. Solar Modulation of the Storm Surge Pattern

[25] The previous analysis is based on a SSP that remains invariable in both HS and LS years. The presence of significant differences in Figure 4a seems to support that the SSP can be regarded as a common favorable regime for HSE occurrence, regardless of solar activity. Nevertheless, the solar modulation of the EOFs described in the previous section suggests that the atmospheric circulation changes with solar activity. Therefore, a similar solar effect could also be expected in the SSP (i.e., there is an additional solar modulation of the large-scale patterns that favor HSEs). This analysis is required to provide a full explanation of the weak linkage between HSEs and the global EOF1 during LS years (Figure 5b).

[26] SSPs under HS and LS activity are shown in Figure 7. The HS-SSP reflects a wave train anomaly structure close to the SSP obtained for the whole record (Figure 4a), except for a small northward shift of the negative center, which is now centered in the British Isles. The LS-SSP is different, however. The negative lobe of anomalies appears farther south, and the positive center over the Scandinavian Peninsula (Azores) intensifies (disappears) in comparison with the SSP. As expected, the mean patterns of HS- and LS-SSP (Figure 7c, shading) closely resemble the SSP. Conversely, the HS-SSP minus LS-SSP difference (Figure 7c, lines) provides a measure of the solar-related asymmetry and reveals deeper low pressures over northern Europe during HS. If Z1000 anomalies are projected onto the solar-based SSPs in Figure 7 for HS and LS years separately, the temporal scores so reconstructed show better correlations with the time series of HSEs (r_{HS} = 0.49, $p < 0.01$; r_{LS} = 0.40, $p < 0.1$) than do the global SSP (r_{HS} = 0.47, $p < 0.01$; r_{LS} = 0.27, p = not significant) for both HS and LS periods. The increase in correlations is especially remarkable during LS years, suggesting that the global SSP signature mostly arises from HS activity periods. In contrast, HS years exhibit a robust surge pattern, as revealed by the wide region with significant differences in Figure 7a, but there are not very clear or well-established conditions conductive to HSE during LS years. Therefore, SSP-related modes (i.e., EOF1 for all years or, alternatively, EOF2 for LS years) do not significantly enhance the likelihood of HSE occurrence in LS years.

[27] Despite differences found between solar-based SSPs, the main conclusions drawn in the previous section regarding the disagreement between LS-EOF and favorable conditions for HSE occurrence still apply, and they do not depend on the possible tendency for the global SSP to show specific features of HS years. Thus, the HS-SSP is still strongly associated with HS-EOF1 (PI = 0.69, r^2 = 80.1%). The LS-SSP now fits the LS-EOF2 more poorly and vaguely resembles the LS-EOF1 (Figure 6b), although the dipole is conceptually different and hence, the relationship is far from being significant (not shown). Therefore, the LS-SSP continues to show a pattern that is not supported by any EOF mode.

3.5. Solar Modulation of the Synoptic Patterns Leading to HSEs

[28] To support the hypothesis that the large-scale patterns in Figure 7 in fact reflect synoptic situations, daily composites of Z1000 anomalies relative to the peak of HSEs were performed for HS and LS years. Since the persistence of the synoptic conditions associated with sea surges typically exceeds 5 days [*Trigo and Davies*, 2002], the composites were performed with time lags of up to 5 days preceding the maximum sea level of the HSE.

[29] The peak (lag 0) of the HSE corresponds well with a low-pressure system located in the Gulf of Genoa (not shown), as already pointed out in various studies [e.g., *Trigo and Davies*, 2002; *Lionello*, 2005]. HS and LS patterns do

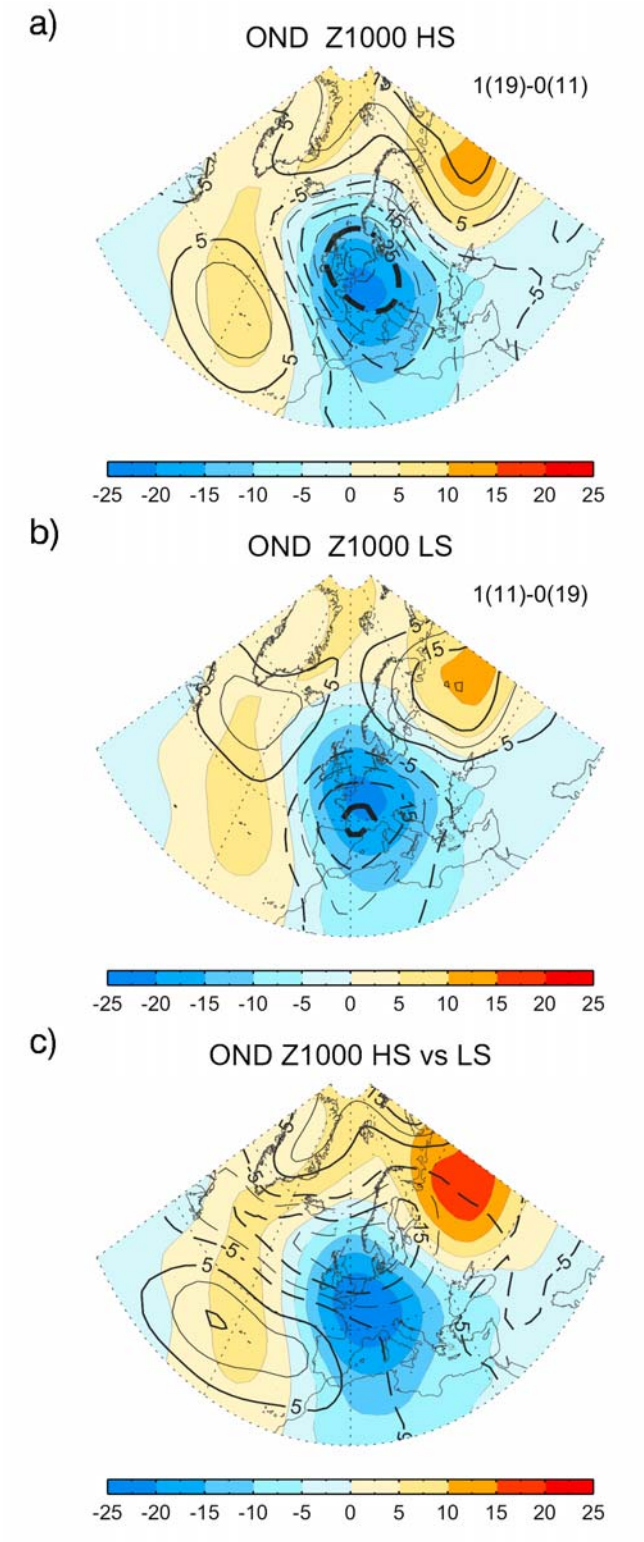

Figure 7. Solar modulation of the seasonal patterns associated with HSEs. As in Figure 4a, but for (a) HS years and (b) LS years. Shaded areas (solid lines) represent the total surge event pattern in Figure 4a (the corresponding pattern of HS and LS years). Bold lines denote differences significant at $p < 0.05$. Solid (dashed) lines indicate positive (negative) differences. (c) The mean (shading) and difference (lines) of HS (7a) and LS (7b) patterns.

not reveal remarkable differences at that time, which suggests that the synoptic patterns are statistically indiscernible immediately before the peak of the HSEs, although there is a tendency for the low pressure to be deeper in HS years (not shown). The differences between HS and LS composites become stronger as the time lag increases, revealing distinctive background conditions for the occurrence of HSE depending on solar activity. Figure 8 shows the synoptic patterns of HS and LS events (shading) and their differences from the total composite of all HSEs (lines) for the 5 day lag. Within that period, the location of the maximum negative departure moved far from the Gulf of Genoa, revealing a NW-SE axis in HS years and a more zonal and southward storm path in LS years. For HS and LS phases the low-pressure system also weakens compared to that at the time

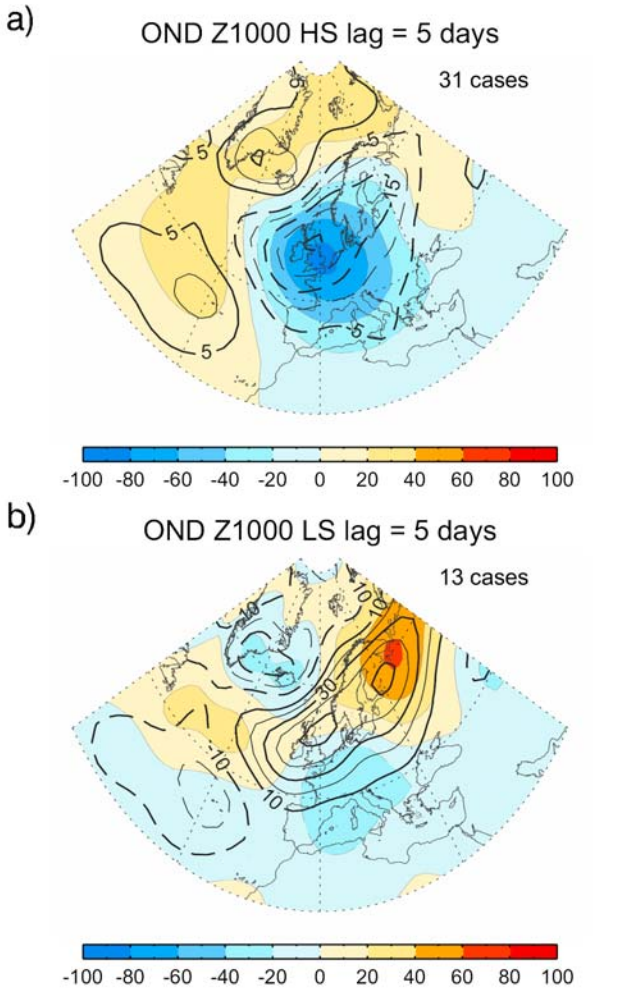

Figure 8. Solar modulation of the synoptic pattern leading to HSEs. Composite of daily Z1000 anomaly fields (shaded areas) for the 5 day lag previous to the peak of HSEs in (a) HS years and (b) LS years. Lines indicate the difference of the given composite from the composite obtained for all years. Solid (dashed) lines indicate positive (negative) differences with a CI of (a) 5 gpm and (b) 10 gpm. Anomalies were computed as departures relative to the daily mean for the 1948–2008 period.

of the peak but this happens at a faster rate during LS years. Note that HS and LS synoptic patterns resemble their seasonal counterparts in Figure 7. Furthermore, the differences between the specific solar composite and the one computed for all cases arise in the form of the climatological asymmetry obtained in Figure 7c, supporting a fair correspondence between seasonal and synoptic patterns.

[30] *Lionello* [2005] found that a distinction of the synoptic patterns responsible for surge events (a 70 cm threshold was adopted) can be established in terms of the location of the storm with respect to the Alps. For cyclones following a northward path over central and northern Europe, the associated surge level was higher than for cyclones taking a southward path, probably owing to a positive interaction with the orographic forcing of the Alps, which tends to favor the development of a secondary minimum in the lee of the Alps, typically observed in HSEs [e.g., *Trigo et al.*, 1999]. *Trigo and Davies* [2002] also stated that a northward European cyclone track induces the favorable wind channeling along the Adriatic that precedes Venice flooding. These results provide a conceptual, although somewhat hypothetical, framework into which the effect of the solar cycle on the floods of Venice can be placed at synoptic time scales. According to this, a pattern such as that observed in LS years, when storm tracks reveal a preferred southward path, would be less prone to yield high sea levels and hence to a high frequency of HSEs.

4. Discussion

[31] The differences between HS and LS activity in terms of the dominant modes of variability, nonlinearity between the patterns favorable for HSE occurrence, and their mutual relationships suggest a detectable but indirect role of solar activity in the decadal modulation of HSE frequency. The statistical linkages identified in this study are robust; they could be obtained without crucially different results if other criteria were adopted. The analysis described in sections 3.2 and 3.3 has been repeated on a bimonthly basis (i.e., considering the October–November and November–December time periods) to cope partially with the relative high intraseasonal variability of the analyzed region. Results (not shown) are similar to those obtained for the whole season: The SSP and EOF patterns are similar to those shown in Figure 4; the PC1 distribution is similar to that shown in Figure 5; and the SSP-related EOF corresponds to the first mode in HS years and to secondary, less recurrent modes during LS years, as discussed in section 3.3. The analysis has also been repeated with a classification based on the upper and lower terciles of solar activity, leading to 20 years of high, neutral, and low solar activity phases. Results revealed little changes, with a tendency for the linkages to become more significant when the tercile solar definition was employed. In addition, years in which the tercile stratification indicated a neutral phase showed an intermediate behavior between opposite solar activity phases.

[32] From the point of view of a solar modulation of the dominant modes of variability, atmospheric variability (EOF1) was found to be organized in a different way in HS and LS years, a propagating wave train dominating in the former and a meridional dipole emerging in the latter. The patterns that trigger HSE under HS and LS seem to respond accordingly, being somewhat accommodating, although to different degrees, to their respective main modes of atmospheric variability. Consequently, the HS-SSP, the storm surge pattern under HS periods, shows a preference for a penetration axis through northern Europe, resembling HS-EOF1, whereas the LS-SSP reveals an enhancement of a southward path of low-pressure systems, which is neither as robust as nor supported by any mode with an appreciable fraction of explained variance.

[33] The major mode of atmospheric variability enhances HSE occurrence during HS years, via an SSP-EOF link that is destroyed in solar minima. This conclusion does not depend on assuming common or different SSPs and global or solar-separated EOFs. However, the arguments presented in sections 3.3 and 3.4 suggest that atmospheric circulation depends on solar activity. In other words, the higher frequency of HSEs during HS years cannot be explained as simply a solar effect in the recurrence of a solar-invariant spatial pattern (EOF1 and the SSP, described in section 3.2) that is favorable for HSE occurrence. Rather, the spatial characteristics of the atmospheric variability (EOF) and the specific conditions for HSE occurrence (SSP) seem to depend on solar activity, and only in HS periods is there a strong similarity between HS-EOF1 and HS-SSP.

[34] The results presented herein provide statistical evidence of a solar influence in the frequency of HSEs based on a consistency between the patterns that trigger HSEs and the atmospheric circulation regimes (EOFs) associated with them. Although the physical mechanisms behind these linkages are unknown, the existence of a solar effect in tropospheric weather regimes is supported by previous studies. In terms of storminess, the EOF1 patterns reflect a preferred northward path of storm track activity over northern Europe in HS years that shifts southward toward the Iberian Peninsula during LS years. This is in agreement with the solar asymmetry found in the patterns favorable for HSE occurrence. A similar northward displacement of the storm track at solar maximum has also been suggested for the winter season [e.g., *Gleisner and Thejll*, 2003]. In contrast, the differences observed between EOF1 in HS and EOF1 in LS years are in agreement with the results of *Kodera* [2003]. *Kodera* reported that during LS winters, the NAO pattern already arises in late autumn as the classical seesaw pressure pattern confined to the Atlantic, whereas in HS winters the NAO originates from the Eurasian sector in late autumn, to form a more hemispherical NAO pattern at the beginning of the winter. *Kodera and Kuroda* [2005] suggested that the origin of the solar activity influence in the spatial structure of the NAO lies in the stratosphere. According to them, stratospheric signatures extend downward to the troposphere in HS years through interaction with planetary waves, whereas during LS phases, when wave activity is relatively unperturbed, the downward propagation is weak and regional-scale features dominate in the troposphere. Similar dynamical processes may be involved in changes in the spatial patterns reported herein, provided that solar signals in the extratropics may be detected as early as in October [e.g., *Baldwin and Dunkerton*, 2005].

[35] It should also be stressed that solar effects similar to those reported here for the frequency of HSEs have not reliably been identified in previous studies, which were focused on past multidecadal periods of anomalous solar

activity (e.g., the Maunder minimum [*Camuffo et al.*, 2000; *Camuffo and Sturaro*, 2004]. The relatively short period of analysis considered in this study does not allow for excluding the possibility that the statistical linkage reported here arises from a random sequence during three solar cycles from the 1970s to 1990s. Alternatively, the relationship could not be stationary, as suggested by the wavelet spectrum in Figure 2, nor could it be masked by other factors at time scales longer than the 11 year solar cycle, as hypothesized by *Camuffo et al.* [2000].

[36] On the contrary, the presence of an 11 year modulation found in this study and the absence of an effect caused by decadal periods of low solar activity in the past are puzzling, but not necessarily logically inconsistent. The 11 year modulation introduces a small, but detectable, perturbation of the present climate regime, whereas persistent periods of anomalous solar activity such as observed in the past (with eventually different spectral characteristics with respect to the 11 year cycle) might have introduced a much larger shift of the circulation, thus setting a different climate regime. The effects of such a relatively large shift on a local process (the storm surge in Venice) would be quite different from those of a small perturbation of the present circulation. Uncertainties in the past records of sunspots, due to subjective estimates and the lack of a quantitative physical dependence on solar irradiance [*Vaquero*, 2007], could also be a factor obscuring the linkage between solar activity and surge events in the past.

[37] Finally, the discrepancy with previous studies at centennial time scales could also arise from the definition of surge events. As stated in section 2, surge events are defined here as those episodes whose strength exceeds the 95th percentile of the event distribution. Thus, only HSEs are taken into account. For weaker surge events (below the 90th percentile) the signal decreases and, eventually, becomes nonsignificant. If the link with solar flux is restricted to HSEs, rather than to all surge events in general, it is not surprising that previous studies did not find significant relationships when all surge events were considered. Note that the confinement of the solar signal to HSEs points to an unknown, strongly nonlinear, physical mechanism, the identification of which is clearly essential for the validity of the statistical analysis carried out in this study, and which is triggered only when events cross a minimum threshold. Further analyses are required to explain these uncertainties and to provide a more definitive dynamical explanation of the role of solar activity in HSEs.

5. Conclusions

[38] In this study the long-term variability of autumn HSEs in Venice is addressed for the period 1948–2008. A significant decadal variability is found, in good correspondence with the 11 year solar cycle, with HS years revealing significant increases in the frequency of OND HSEs.

[39] Solar activity is suggested to exert an indirect influence on the likelihood of HSE occurrence by modulating the dominant modes of variability, the patterns responsible for HSEs, and their mutual relationships, so that a constructive interaction between them is attained only during solar maxima. From a large-scale perspective, solar activity modulates the spatial patterns of atmospheric variability, such that a propagating wave train dominates in HS years and a more meridional dipole, characteristic of a southward shift of storm tracks, increases in LS periods. Within this general background, the patterns that enhance high surge activity under HS and LS years change according to their respective main modes of atmospheric variability but to different extents. Thus, whereas the HS-SSP is robust and significantly favored by the first mode of regional variability during HS years, the corresponding LS-SSP in LS years is less clear and is not associated with any complementary mode of atmospheric variability. As a consequence, the large-scale regime conducive to a high frequency of HSEs is statistically more frequent in HS years than in LS years, during which no single mode is able to fully meet the favorable conditions triggering HSEs. These results suggest that (1) specific atmospheric regimes, other than those raised by the general modes of variability, are required to establish the proper background for HSE occurrence during solar minima; (2) no robust patterns or univocal signatures enhance HSE occurrence in solar minima.

[40] The distinctive solar-related large-scale patterns are mirrored in the settlement of synoptic conditions preceding the peak of HSEs. Thus, under HS conditions, HSEs are triggered by deeper low-pressure systems with storm track enhancement over northern Europe and a NW-SE penetration axis into the Mediterranean. Under LS conditions, HSEs are preceded by weaker and southward-shifted low-pressure anomalies and a preference for a more zonal path throughout the Iberian Peninsula, which is not strongly involved in HSEs.

[41] **Acknowledgments.** NCEP reanalysis data were provided by the NOAA/OAR/ESRL PSD, Boulder, Colorado, at their Web site (http://www.cdc.noaa.gov/). The Ufficio Idrografico of Venice provided sea level data. Solar data were obtained from the National Geophysical Data Center of the NOAA at their Web site (www.ngdc.noaa.gov/stp/SOLAR/ftpsolarradio.html). This study was partially supported by EU Sixth Framework Program (CIRCE) contract 036961 (GOCE) and the ENAC project (PTDC/AAC-CLI/103567/2008) funded by the IDL-FFCUL. We also acknowledge the contribution from the ESF MedCLIVAR program.

References

Ammerman, A. J., and C. E. McClennen (2000), Saving Venice, *Science*, *289*(5483), 1301–1302, doi:10.1126/science.289.5483.1301.

APAT (2006), Aggiornamento sulle osservazioni dei livelli di marea nella laguna di Venezia, Rapporto no. 69/2006, Agency for Environmental Protection and Technical Services, Venice.

Baldwin, M. P., and T. J. Dunkerton (2005), The solar cycle and stratosphere-troposphere dynamical coupling, *J. Atmos. Sol. Terr. Phys.*, *67*, 71–82, doi:10.1016/j.jastp.2004.07.018.

Balling, R.C., and S. S. Roy Jr. (2005), Analysis of spatial patterns underlying the linkage between solar irradiance and near-surface air temperatures, *Geophys. Res. Lett.*, *32*, L11702, doi:10.1029/2005GL022444.

Barnston, A. G., and R. E. Livezey (1987), Classification, seasonality and persistence of low-frequency atmospheric circulation patterns, *Mon. Weather Rev.*, *115*, 1083–1126, doi:10.1175/1520-0493(1987)115<1083:CSAPOL>2.0.CO;2.

Barriopedro, D., R. García-Herrera, and R. Huth (2008), Solar modulation of Northern Hemisphere winter blocking, *J. Geophys. Res.*, *113*, D14118, doi:10.1029/2008JD009789.

Camuffo, D. (1993), Analysis of the sea surges at Venice from A.D. 782 to 1990, *Theor. Appl. Climatol.*, *47*, 1–14, doi:10.1007/BF00868891.

Camuffo, D., and G. Sturaro (2003), Sixty-cm submersion of Venice discovered thanks to Canaletto's paintings, *Clim. Change*, *58*(3), 333–343, doi:10.1023/A:1023902120717.

Camuffo, D., and G. Sturaro (2004), Use of proxy-documentary and instrumental data to assess the risk factors leading to sea flooding in Venice, *Global Planet. Change*, *40*, 93–103, doi:10.1016/S0921-8181(03)00100-0.

Camuffo, D., C. Secco, P. Brimblecombe, and J. Martin Vide (2000), Sea storms in the Adriatic Sea and the western Mediterranean during the last millennium, *Clim. Change*, *46*, 209–223, doi:10.1023/A:1005607103766.

Christoforou, P., and S. Hameed (1997), Solar cycle and the Pacific "centers of action," *Geophys. Res. Lett.*, *24*(3), 293–296, doi:10.1029/97GL00017.

Coughlin, K. T., and K. K. Tung (2004), 11-year solar cycle in the stratosphere extracted by the empirical mode decomposition method, *Adv. Space Res.*, *34*, 323–329, doi:10.1016/j.asr.2003.02.045.

Fagherazzi, S., G. Fosser, L. D'Alpaos, and P. D'Odorico (2005), Climatic oscillations influence the flooding of Venice, *Geophys. Res. Lett.*, *32*(19), L19710, doi:10.1029/2005GL023758.

Gleisner, H., and P. Thejll (2003), Patterns of tropospheric response to solar variability, *Geophys. Res. Lett.*, *30*(13), 1711, doi:10.1029/2003GL017129.

Gleisner, H., P. Thejll, M. Stendel, E. Kaas, and B. Machenhauer (2005), Solar signals in tropospheric re-analysis data: Comparing NCEP/NCAR and ERA 40, *J. Atmos. Sol. Terr. Phys.*, *67*, 785–791, doi:10.1016/j.jastp.2005.02.001.

Huth, R., L. Pokorná, J. Bochníček, and P. Hejda (2006), Solar cycle effects on modes of low-frequency circulation variability, *J. Geophys. Res.*, *111*, D22107, doi:10.1029/2005JD006813.

Kalnay, E., et al. (1996), The NCEP/NCAR 40-year reanalysis project, *Bull. Am. Meteorol. Soc.*, *77*, 437–471, doi:10.1175/1520-0477(1996)077<0437:TNYRP>2.0.CO;2.

Kodera, K. (2002), Solar cycle modulation of the North Atlantic Oscillation: Implication in the spatial structure of the NAO, *Geophys. Res. Lett.*, *29*(8), 1218, doi:10.1029/2001GL014557.

Kodera, K., and Y. Kuroda (2005), A possible mechanism of solar modulation of the spatial structure of the North Atlantic Oscillation, *J. Geophys. Res.*, *110*, D02111, doi:10.1029/2004JD005258.

Labitzke, K. (2005), On the solar cycle-QBO relationship: A summary, *J. Atmos. Sol. Terr. Phys., 67*, 45–54, doi:10.1016/j.jastp.2004.07.016.

Lean, J., and D. Rind (2001), Earth's response to a variable Sun, *Science*, *292*, 234–236, doi:10.1126/science.1060082.

Lionello, P. (2005), Extreme storm surges in the Gulf of Venice: Present and future climate, in Venice and Its Lagoon, State of Knowledge, edited by C. Fletcher and T. Spencer, pp. 59–65, Cambridge Univ. Press, Cambridge, UK.

Matthes, K., Y. Kuroda, K. Kodera, and U. Langematz (2006), Transfer of the solar signal from the stratosphere to the troposphere: Northern winter, *J. Geophys. Res.*, *111*, D06108, doi:10.1029/2005JD006283.

Pirazzoli, P. A. (1991), Possible defenses against a sea-level rise in the Venice area, Italy, *J. Coastal Res.*, *7*, 231–248.

Pirazzoli, P. A., and A. Tomasin (1999), Recent abatement of easterly winds in the northern Adriatic, *Int. J. Climatol.*, *19*, 1205–1219, doi:10.1002/(SICI)1097-0088(199909)19:11<1205::AID-JOC405>3.0.CO;2-D.

Pirazzoli, P. A., and A. Tomasin (2002), Recent evolution of surge-related events in the northern Adriatic area, *J. Coastal Res.*, *18*(3), 537–554.

Robinson, A. R., A. Tomasin, and A. Artegiani (1973), Flooding of Venice, phenomenology and prediction of the Adriatic storm surge, *Q. J. R. Meteorol. Soc.*, *99*(422), 688–692, doi:10.1002/qj.49709942210.

Shindell, D., D. Rind, N. Balachandran, J. Lean, and P. Lonergan (1999), Solar cycle variability, ozone, and climate, *Science*, *284*, 305–308, doi:10.1126/science.284.5412.305.

Smith, R. L. (1986), Extreme value theory based in the n-largest annual events, *J. Hydrol. [Amsterdam]*, *86*, 27–43, doi:10.1016/0022-1694(86)90004-1.

Tapping, K. F., and D. P. Charrois (1994), Limits to the accuracy of the 10.7 cm flux, *Sol. Phys.*, *150*, 305–315, doi:10.1007/BF00712892.

Tomasin, A. (2002), The frequency of Adriatic surges and solar activity, *ISDGM Tech. Rep.*, *194*, 1–8.

Trigo, I. F., and T. D. Davies (2002), Meteorological conditions associated with sea surges in Venice: A 40 year climatology, *Int. J. Climatol.*, *22*, 787–803, doi:10.1002/joc.719.

Trigo, I. F., T. D. Davies, and G. R. Bigg (1999), Objective climatology of cyclones in the Mediterranean region, *J. Clim.*, *12*, 1685–1696, doi:10.1175/1520-0442(1999)012<1685:OCOCIT>2.0.CO;2.

Tsimplis, M. N., and S. A. Josey (2001), Forcing of the Mediterranean Sea by atmospheric oscillations over the North Atlantic, *Geophys. Res. Lett.*, *28*(5), 803–806, doi:10.1029/2000GL012098.

van Loon, H., and D. J. Shea (1991), A probable signal of the 11-year solar cycle in the troposphere of the Northern Hemisphere, *Geophys. Res. Lett.*, *26*, 2893–2896, doi:10.1029/1999GL900596.

Vaquero, J. M. (2007), Historical sunspot observations: A review, *Adv. Space Res.*, *40*, 929–941, doi:10.1016/j.asr.2007.01.087.

Zanchettin, D., P. Traverso, and M. Tomasino (2006), Discussion on sea level fluctuations along the Adriatic coasts coupling to climate indices forced by solar activity: Insights into the future of Venice, *Global Planet. Change*, *50*, 226–234, doi:10.1016/j.gloplacha.2006.01.001.

Zanchettin, D., P. Traverso, and M. Tomasino (2007), Observations on future sea level changes in the Venice lagoon, *Hydrobiologia*, *577*, 41–53, doi:10.1007/s10750-006-0416-5.

D. Barriopedro, CGUL-IDL, Faculdade de Ciências, Ed. C-8, Universidade de Lisboa, Campo Grande, P-1749-016 Lisbon, Portugal. (dbarriopedro@fc.ul.pt)

R. García-Herrera, Departamento Física de la Tierra II, Facultad de Ciencias Físicas, Universidad Complutense de Madrid, Madrid, Spain.

P. Lionello and C. Pino, Department of Material Science, University of Salento, Lecce, Italy.